The Distribution of Cytoplasmic Microtubules throughout the Cell Cycle of the Centric Diatom *Stephanopyxis turris*: Their Role in Nuclear Migration and Positioning the Mitotic Spindle during Cytokinesis

Linda Wordeman, Kent L. McDonald, and W. Zacheus Cande

Departments of Botany and Zoology, University of California, Berkeley, California 94720

Abstract. The cell cycle of the marine centric diatom *Stephanopyxis turris* consists of a series of spatially and temporally well-ordered events. We have used immunofluorescence microscopy to examine the role of cytoplasmic microtubules in these events. At interphase, microtubules radiate out from the microtubule-organizing center, forming a network around the nucleus and extending much of the length and breadth of the cell. As the cell enters mitosis, this network breaks down and a highly ordered mitotic spindle is formed. Peripheral microtubule bundles radiate out from each spindle pole and swing out and away from the central spindle during anaphase. Treatment of synchronized cells with 2.5×10^{-8} M Nocodazole reversibly inhibited nuclear migration concurrent with the disappearance of the extensive cytoplasmic microtubule arrays associated with migrating nuclei. Microtubule arrays and mitotic spindles that reformed after the drug was washed out appeared normal. In contrast, cells treated with 5.0×10^{-8} M Nocodazole were not able to complete nuclear migration after the drug was washed out and the mitotic spindles that formed were multipolar. Normal and multipolar spindles that were displaced toward one end of the cell by the drug treatment had no effect on the plane of division during cytokinesis. The cleavage furrow always bisected the cell regardless of the position of the mitotic spindle, resulting in binucleate/anucleate daughter cells. This suggests that in *S. turris*, unlike animal cells, the location of the plane of division is cortically determined before mitosis.

MICROTUBULES play a key role in organizing the internal architecture of the cell. They are involved in the rearrangement of cytoplasmic contents (38), and in the establishment of overall cell polarity (20, 49). Microtubules derived from the mitotic spindle participate in the localization of the cleavage furrow in animal cells (40), and in the formation of the cell wall in plant cells (19). To investigate the role of microtubules in these processes it is of primary importance to be able to visualize the overall distribution of cytoplasmic microtubules. In recent years, immunofluorescence microscopy using antibodies to tubulin and improvements in electron microscopy resulting from better preservation of the cytoskeleton have provided a great deal of information about the spatial distribution of cytoplasmic microtubules. These methods, however, are technically difficult to apply to many types of cells, particularly large, yolky, or thickly walled cells. In addition, some cells that are structurally well suited for indirect immunofluorescence exhibit very little spatial and temporal organization of cell cycle events at the level of the light microscope. This makes it difficult to study the functional relationship between the changes that take place in the microtubule distribution of the cell and the cell cycle-specific events that are mediated by microtubules.

The marine centric diatom *Stephanopyxis turris* exhibits an orderly and predictable progression of events throughout its asexual cell cycle, some of which are identifiable at the level of the light microscope by changes in nuclear position (22, 23, 50). In addition, because the siliceous cell wall is perforated by numerous tiny pores, *S. turris* cells can be rendered permeable to antitubulin antibodies by a simple detergent extraction procedure performed after fixation. This technique does not involve the use of enzymatic digestion or other harsh techniques usually used to permeabilize plant cell walls. Despite the fact that plant cells provide good model systems for the participation of cytoplasmic cytoskeletal arrays in intracellular motility (6), cytoplasmic localization (2, 3), and morphogenesis (17, 20, 29), the difficulties involved with fixation and permeabilization of plant cells have, with a few exceptions (10, 14, 15, 58), resulted in a dearth of immunofluorescence studies of the plant cytoskeleton.

There are five morphologically distinct events that take place during the cell cycle of *S. turris*, several of which involve microtubules. First, ~2–3 h before mitosis, the nuclei in

adjacent sister cells migrate in a symmetrical manner from the hypothecal valve (end wall), where they have been located throughout most of interphase, to the center of girdle band region of the cell. This migration takes place concurrently with cell elongation and our immunofluorescence and drug studies imply significant participation of microtubules in this process. Secondly, the centered nuclei undergo karyokinesis using a structurally highly ordered mitotic spindle. Third, a broad cleavage furrow forms during cytokinesis separating the two daughter cells. Unlike the situation in higher plants and most algae, this event does not use microtubules such as the phycoplast or phragmoplast microtubule systems that have been described (19). Within an hour after cytokinesis, the daughter cells have completed the construction of new hypothecal valves (end walls). The morphology of these new walls can be distorted by the application of microtubule inhibitors during their synthesis (27, 44). Finally, during interphase, the cells synthesize siliceous girdle bands which will be incorporated into the existing cell wall as extensions of the valve to facilitate the relatively sudden increase in cell size that takes place before the next cell division.

Studies of animal cells have demonstrated that displaced mitotic spindles can establish cleavage furrows (9, 40). Moreover, displaced nuclei in higher plants can induce secondary cell walls and can influence the shape and orientation of the growing cell plate (3, 5, 19, 31, 46, 54). However, several observations suggest that plant cells anticipate the plane of cleavage using a cortical determinant established before mitosis (7, 8, 19, 32, 45, 54, 55, 58). We have used the microtubule inhibitor nocodazole to study the extent to which the mitotic spindle influences the location of the cleavage plane in *S. turris*. We show here that nocodazole reversibly inhibits nuclear migration and can be used to induce karyokinesis before the completion of nuclear migration resulting in spindles which are displaced toward the hypothecal end of the cell. Surprisingly, we find that displacement of mitotic nuclei results in complete spatial uncoupling of karyokinesis from cytokinesis. This demonstrates that in *S. turris* the location of the presumptive cleavage furrow is not determined by the position of the spindle but is cortically determined before mitosis. Nocodazole-induced displacement of mitotic nuclei will neither alter the position of the original furrow nor induce additional furrows. We present indirect immunofluorescence studies illustrating this phenomenon.

Materials and Methods

Cell Culture and Handling

S. turris (stock #L1272) was obtained from the Culture Collection of Marine Phytoplankton, Bigelow Laboratory for Ocean Services, West Boothbay, ME. Cells were grown in F/2 medium (18) in a suspension culture on a 6.5-h light, 17.5-h dark schedule at 19°C. Cells were drugged for 3 h with either 2.5×10^{-8} M or 5.0×10^{-8} M nocodazole (Sigma Chemical Co., St. Louis, MO) after which time the cells were collected on 60-μm mesh filters and washed extensively to remove the drug. To score the cells for nuclear position, aliquots of the cell suspension were collected and fixed with 3.7% formaldehyde, 5% acetic acid in F/2 for 30 min, then suspended in isotonic buffer (487 mM NaCl, 26.1 mM KCl, 4.35 mM Tris [pH 8.0], 0.87 mM EGTA) plus 1 μg/ml 4,6-diamidine-2-phenylindole dihydrochloride (DAPI)[1] (Sigma Chemical Co.), to stain the chromatin.

1. *Abbreviations used in this paper*: DAPI, 4,6-diamidine-2-phenylindole dihydrochloride; MTOC, microtubule-organizing center.

Indirect Immunofluorescence

The antibody against tubulin (a monoclonal against sea urchin flagellar tubulin) was kindly provided by Dr. David Asai (Department of Biology, Purdue University) and its preparation and characterization have been described previously (1). Cells were fixed in 0.5% glutaraldehyde for 30 min and immediately extracted with 0.1% Triton X-100 in phosphate-buffered saline (PBS), pH 7.4, plus 0.12% Azide for several hours to overnight at 20°C. Although it is possible to visualize microtubules without extensive detergent pretreatment, the long extraction times reduced chloroplast autofluorescence without perceptibly altering the microtubule distribution. This suggested to us that rearrangement of microtubules due to disruption of membranes is not a serious problem using this procedure. Extracted cells were reduced in 1 mg/ml sodium borohydride (Sigma Chemical Co.) in 1:1 PBS/methanol for 20 min. After extensive PBS rinses the cells were incubated in primary antibody for 24 h at 20°C then washed in PBS containing 1 μg/ml DAPI. The cells were incubated for a similar length of time in fluorescein-conjugated goat anti-mouse IgG (Cappel Laboratories, Cochranville, PA), washed, and then mounted under coverslips in 90% glycerol, 10% PBS, 100 mg/ml 1,4 diazobicyclo-(2,2,2)octane plus 45-μm latex beads (Ernest F. Fullam, Inc., Schenectady, NY) to keep the coverslip elevated over the cells.

Fluorescence Microscopy

Stained cells were photographed with Kodak Technical Pan SO-115 film using a Zeiss Photoscope III and Zeiss filter sets 48 77 16 and 48 77 02. Autofluorescence due to residual photosynthetic pigments in the chloroplasts was apparent particularly at the red wavelengths. This contributed to background fluorescence in monochrome micrographs.

Electron Microscopy

Intact cells were fixed in 0.5% glutaraldehyde in F/2 medium for 30 min at 23°C (unless otherwise stated, all remaining steps were at 23°C). Cells were rinsed in PBS, pH 7.3, postfixed in 0.2% OsO_4 + 0.3% $K_3Fe(CN)_6$ in PBS for 15 min at 4°C. The cells were then rinsed in PBS, followed by distilled H_2O and then incubated in 2% aqueous uranyl acetate for 90 min. After dehydration in acetone by 10% steps for 10 min each, the cells were embedded in Epon-Araldite (3.1 gm Epon 812; 2.2 gm Araldite 502; 6.1 gm DDSA; and 0.2 mg DMP-30). Sections ~75 nm thick were pushed up on slot grids, stained for 10 min in 1% aqueous uranyl acetate, 5 min in alkaline lead citrate, and then viewed in a JEOL 100S electron microscope at 80 kV.

Results

Microtubule Distribution throughout the Cell Cycle

After each cell division in *S. turris*, the daughter nuclei are located opposite each other against the newly formed end walls (hypotheca) of the two adjacent daughter cells (Fig. 1). They remain in this position throughout most of interphase.

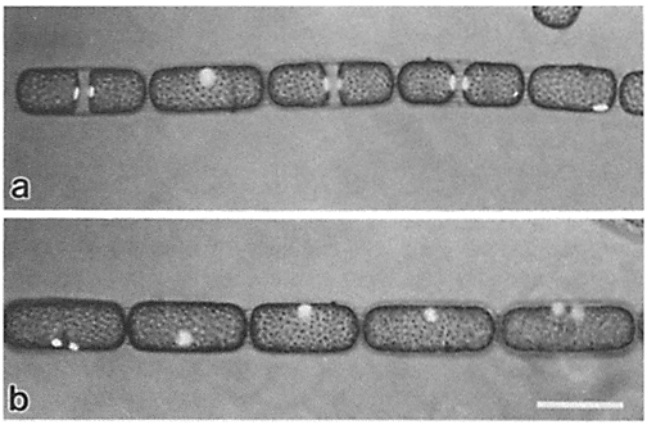

Figure 1. Strands of DAPI-stained *S. turris* cells in different stages of nuclear migration and mitosis. (*a*) The farthest cell to the right is in nuclear migration. The nucleus is completely centered in the second cell from the left and on either side of this cell there are newly cleaved sister cell pairs. (*b*) A strand of mitotic cells. Bar, 100 μm.

The nucleus, microtubules, and other cytoplasmic organelles are located in the thin layer of cytoplasm that surrounds the large central vacuole. Transmission electron microscopy shows a system of cytoplasmic microtubules radiating out from a multi-layered structure in a depression on the face of the interphase nucleus (see Fig. 3 *a*). Indirect immunofluorescence microscopy shows that the microtubules extend unbroken along the entire length of the cell, parallel to the cell's longitudinal axis, and terminate near the opposite end wall or epitheca (see Fig. 2 *a*). About 3 h before the onset of the next cell division the nuclei of adjacent sister cells migrate in symmetrical paths to the center of each cell, concurrent with a rapid increase in cell length (see Figs. 1, 2, and 5).

During nuclear migration microtubules can be seen radiating from a microtubule-organizing center (MTOC) that is close to the nucleus and stains brightly with the antitubulin antibodies (Fig. 2, *b–e*). The microtubules form a network around the nucleus and radiate in all directions often extending much of the length or breadth of the cell. At certain levels of focus, bundles of microtubules can be seen emanating from either side of the MTOC and extending preferentially in either direction along the path of nuclear migration (Fig. 2 *d*). A thin section through the MTOC of a migrating nucleus is shown in Fig. 3 *b*. At this stage the MTOC is composed of two multi-layered plates from which extend two spatially distinct classes of microtubules. A tube of close-packed microtubules extends between the two plates. Other microtubules extend out from the two plates, often crossing each other at an angle, and continuing through nuclear envelope–lined channels into the adjacent chromatin mass. Double-labeling experiments with antitubulin and antibodies specific to spindle pole proteins that label the plates demonstrate that it is the area between the plates that stains brightly with antitubulin (Wordeman, L., and J. L. Salisbury, unpublished results). Finally, there are between two and four large vesicles associated with the distal face of each plate (Fig. 3, *b* and *c*).

Soon after the nucleus reaches the center of the cell (girdle region) the cytoplasmic microtubules disappear, the nucleus becomes more rounded and the nucleolus breaks down. Condensed prophase chomosomes are visible at this time in DAPI-stained preparations. The MTOC subsequently assumes the form of a short central spindle with some peripheral microtubule bundles extending out into the nucleus (Fig. 4 *a*). In the metaphase cell, the closely packed bundles of microtubules that comprise the central spindle can be clearly distinguished from the peripheral bundles of microtubules that angle outward from the spindle poles into the surrounding chromatin (Fig. 4, *b–d*). The spindle continues to increase in length and breadth throughout metaphase while the chromatin maintains its highly organized metaphase configuration (Fig. 4 *b*, inset). The transition from metaphase to anaphase is difficult to determine in these cells due to the large amount of chromatin surrounding the spindle. As the central spindle elongates, the peripheral microtubule bundles swing outward and away from the cell center (Fig. 4, *c* and *d*). By late anaphase, the chromatin masses have separated completely and the peripheral microtubules are angled outward from the poles like an umbrella that has been blown inside-out. The peripheral microtubule bundles in telophase cells are longer, thinner, and more numerous than those of earlier stages. They extend from the pole region back into the cytoplasm (Fig. 4 *e*). The

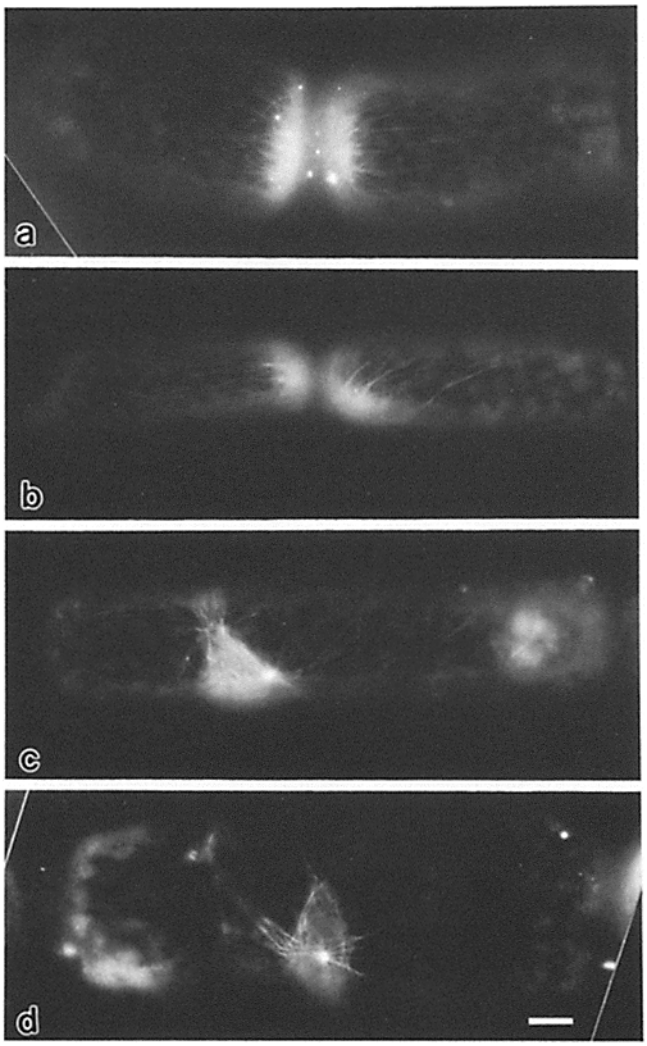

Figure 2. Antitubulin immunofluorescence microscopy of *S. turris* cells in interphase (*a*) and nuclear migration (*b–d*). Note the brightly staining MTOC in *c* and *d*. Background autofluorescence from chloroplast pigments allows visualization of the overall cell shape. Bar, 10 μm.

area of the pole that serves as attachment points for the proximal ends of the peripheral microtubules is a ring or doughnut-shaped region in photographs exposed for shorter time periods (Wordeman, L., and J. L. Salisbury, unpublished data).

The cleavage furrow in these organisms is broad (20–30 μm). It is traversed by a microtubule bundle equivalent to a midbody that is lost within an hour after cytokinesis is completed (Fig. 4 *f*). The interphase microtubule network appears to be almost completely reestablished by the end of cytokinesis. The complete cell cycle–specific distribution of microtubules is summarized in the cartoon in Fig. 5.

Effect of Nocodazole on Nuclear Migration and Cell Division

Cultures of *S. turris* grown under a strict light-dark cycle (6.5-h light, 17.5-h dark) are naturally synchronous (see Fig. 6 *a*). The cells begin nuclear migration ~1 h before the end of the light period, or 5.5 h on a 24-h clock. By the start of the dark period (6.5 h), the proportion of cells with centered nuclei is

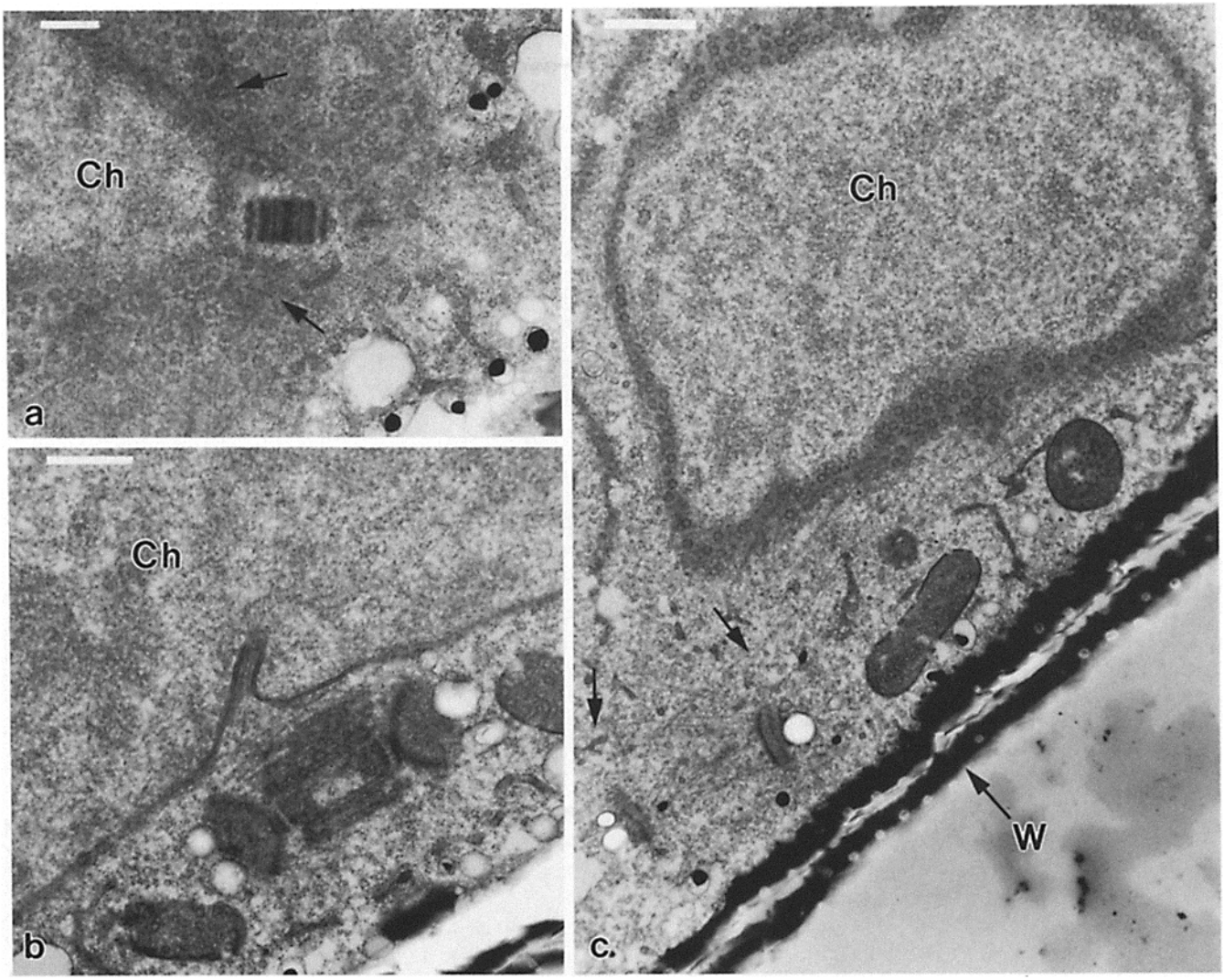

Figure 3. Transmission electron micrographs of the MTOC before (*a*) and during nuclear migration (*b* and *c*). (*a*) The MTOC, which lies in a depression on the surface of the interphase nucleus, is centrally located againt the hypothecal end wall of the cell. Microtubules radiate out from the MTOC (arrows). The close-packed rings are nuclear pores. Bar, 0.5 μm. (*b*) Microtubules extend between the plates of the MTOC and also into channels in the nuclear membrane. Bar, 0.5 μm. (*c*) Lower magnification of a later-stage MTOC and nucleus. Microtubules (arrows) extend in opposite directions from the inner face of each plate, crossing over each other in the region between the arrows. Bar, 1 μm. *Ch*, chromatin; *W*, cell wall.

rising concurrent with a decline in the number of cells that have not completed nuclear migration. The peak in the number of cells with centered nuclei, which is followed closely by an increase in numbers of recently divided cells, shows that the cells pass through a natural maximum level of mitotic activity between 7.5 and 8.5 h. We have found that the proportion of cells in this mitotic peak varies from day to day but that the timing of the peak remains constant.

We examined the effect of the microtubule inhibitor nocodazole on nuclear migration and mitosis by exposing the cells to a 3-h pulse of 2.5×10^{-8} M nocodazole from 5.5 to 8.5 h (Fig. 6*b*). Microtubule-containing structures reappear within minutes after the drug is washed out and replaced with fresh medium (see next section). We refer to this procedure as "reversal." We found that exposure to 2.5×10^{-8} M nocodazole increased the amount of time that the cells spent in nuclear migration. Cells with off-center nuclei accumulated steadily throughout the drug exposure period without completing mitosis unlike the progression of events observed in the control cells. At reversal, the proportion of cells in nuclear migration falls by ⅔ within 30 min. In addition, the proportion of recent dividers, which had been at a low level during the drugging period, rises quickly after 30 min. Independent experiments using in situ immunofluorescence and in vitro spindle isolations from drugged cells have shown that the accumulation of mitotic spindles is greatest between 15 and 20 min after reversal. The post-reversal peak in the number of cells with centered nuclei is not very high. We feel that this is attributable to two phenomena. First, after drug reversal the nuclei have only a very short time to reach the center of the cell before completing cell division. Therefore, it is likely that the nuclei of drug-treated cells spend very little time in the centered position compared to the control cells. Secondly, we have found that a small percentage of the cells exposed to nocodazole can form perfectly normal, functional spindles that are not located in the center of the cell. Both of these

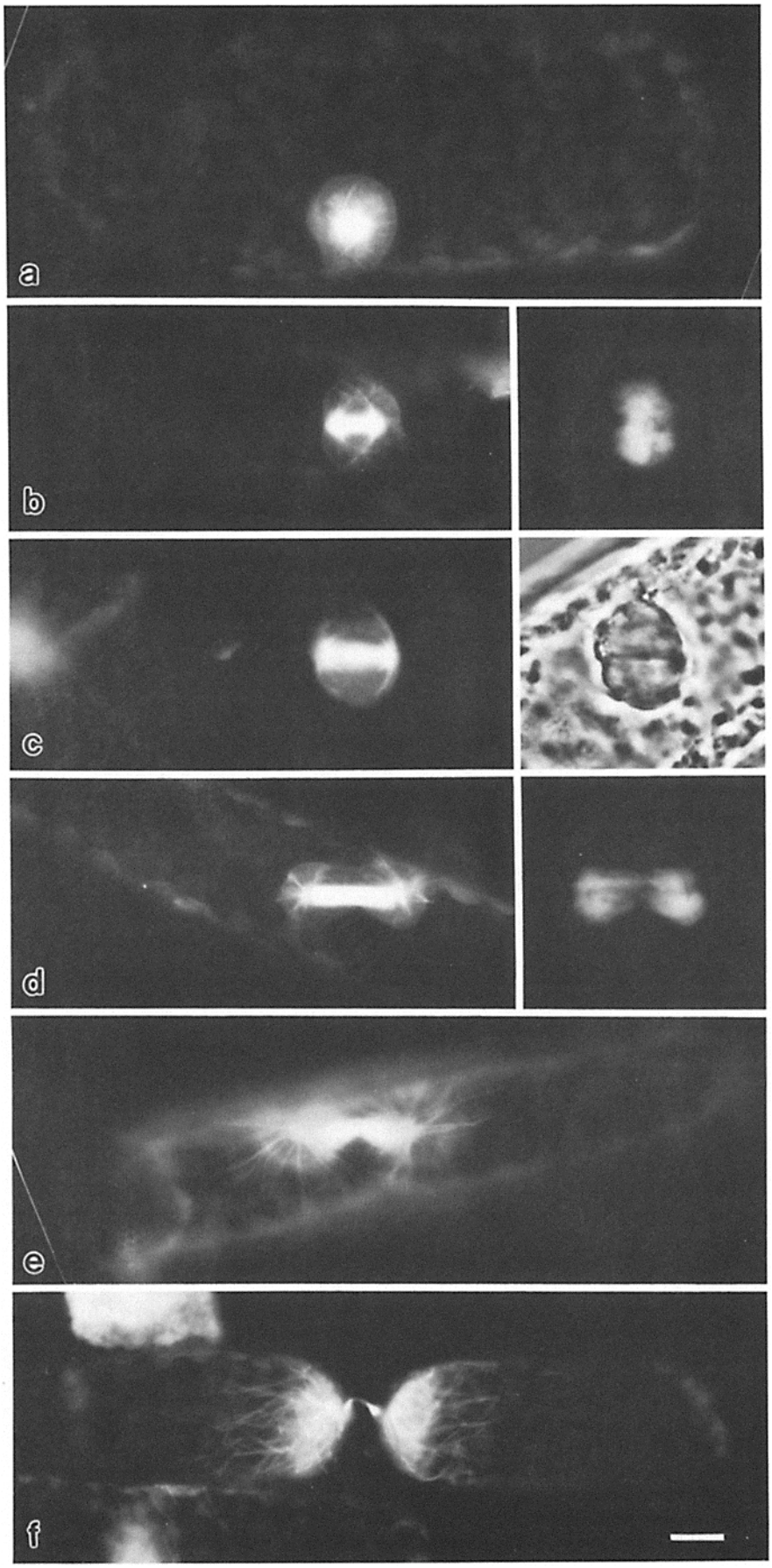

Figure 4. Antitubulin immunofluorescence microscopy of *S. turris* showing successive stages of mitosis. (*a*) Prometaphase. All the interphase microtubule arrays have been withdrawn from the cytoplasm. Photographic exposures favoring reproduction of the small peripheral microtubules in the chromatin result in overexposure of the central spindle in cells at this stage. (*b*) Metaphase. Central and peripheral microtubules can be distinguished. Inset shows DAPI-stained chromatin in the same cell. (*c*) Peripheral microtubules swing back at early anaphase. Inset shows the same cell in phase. (*d*) Late anaphase cell. Inset shows DAPI-stained chromatin. (*e*) Peripheral microtubules establish extensive arrays during telophase although there is still a distinct central spindle. (*f*) Midbody and cytoplasmic microtubule arrays just after cytokinesis. In contrast to the cells in Fig. 2 *a*, these daughter cells are spaced far apart, characteristic of recently divided cells, and cell wall deposition has not yet taken place. Bar, 10 μm.

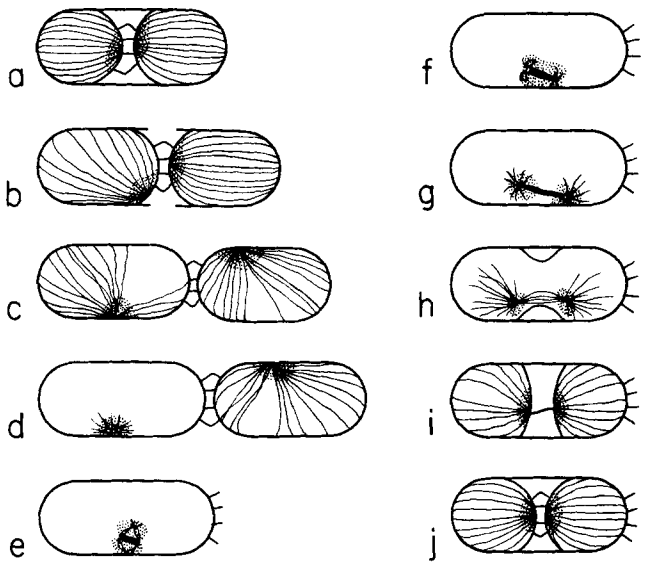

Figure 5. Cell cycle–specific microtubule distribution in *S. turris*. Stippling indicates the nucleus. (*a*) Interphase sister cell pair. (*b–d*) Successive stages of symmetrical nuclear migration. Cell elongation occurs at the same time. (*e*) Metaphase. (*f*) Anaphase. (*g*) Telophase. (*h*) Cytokinesis. (*i*) Recently divided cell prior to cell wall synthesis. (*j*) Cell wall synthesis complete. Accurate nuclear position and cell size have been adapted from films of dividing *S. turris* cells (23).

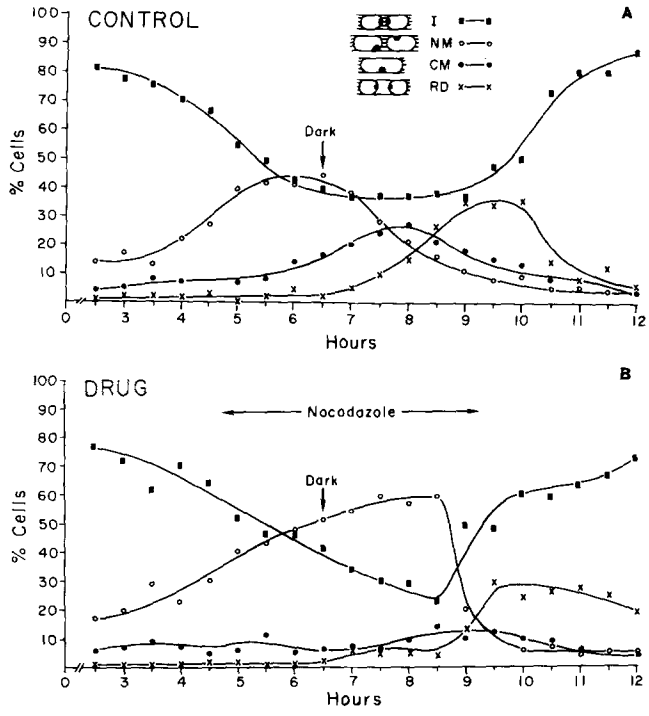

Figure 6. Graphs of nuclear position versus time in (*a*) a control population and (*b*) cells treated with 2.5×10^{-8} M nocodazole. (■) Interphase. (○) Nuclear migration. (●) Centered and mitotic. (×) Recently divided.

phenomena are discussed in greater detail in the following sections. These experiments suggest that exposure to low concentrations of nocodazole can inhibit nuclear migration and cell division and that this effect is reversible.

Indirect Immunofluorescence of Nocodazole-treated Cells

Using indirect immunofluorescence we examined the effect of nocodazole on the cell cycle–specific microtubule distribution at two different drug concentrations. One batch of cells was exposed to a 3-h pulse of 2.5×10^{-8} M nocodazole which, as we have demonstrated above, gives us good reversal. A second batch of cells from the same culture was pulsed with 5.0×10^{-8} M nocodazole, a concentration which we have found gives us poor reversal; i.e., no post-reversal peak of recent dividers (data not shown). The results are summarized in Fig. 7.

Cells that were exposed to 2.5×10^{-8} M nocodazole and then fixed before reversal contain small MTOC-like structures and thin needles that are closely associated with the nucleus and that stain brightly with the tubulin antibody. Some of these thin bundles stain more brightly in the center, reminiscent of the overlap zone of normal spindles. We do not see any cytoplasmic microtubule arrays associated with the off-center nuclei or the MTOC-like structures (Fig. 7, *a* and *b*). 20 min after reversal, 69% of the cells contain normal-appearing metaphase spindles, and microtubules can be seen emanating from the brightly staining MTOCs in the remaining 31% of the cells (Fig. 7, *c* and *d*).

After a 3-h pulse of 5.0×10^{-8} M nocodazole, most of the cells do not contain any organized antitubulin staining structures. A small population of cells contain a tiny, dimly staining dot in the same position that one would expect a find the MTOC in the migrating nuclei of undrugged cells (Fig. 7, *e* and *f*). 20 min after reversal, most of the cells contain structures that stain brightly with antitubulin. A proportion (40%) of the cells contain normal-appearing cytoplasmic microtubules extending from an MTOC associated with the nucleus and also from the nuclear pole of the cell in cells where the nucleus has not yet begun to migrate. The remaining 60% of the cells contain many brightly staining bundles of microtubules pointing in random directions within the condensed chromatin (Fig. 7, *g* and *h*). We call these disorganized bundles splayed spindles. The cells with splayed spindles give rise to daughter cells containing between two and six unequally sized chromatin masses unlike the control cells which contain regular spindles and divide normally.

The proportion of cells exposed to two different levels of nocodazole with nuclei in either the interphase, off-center, or centered position are compared in Table I. A large percentage of the cells exposed to 5.0×10^{-8} M nocodazole accumulate in the off-center position, or migratory phase. Although these cells reform microtubule-containing structures after reversal, most of these structures are abnormal (see above) and by 20 min after reversal, very few of the nuclei have centered. In contrast, a substantial percentage of the cells exposed to 2.5×10^{-8} M nocodazole are already in the centered position by reversal time and this number increases significantly by 20 min post-reversal. This suggests that the lower concentration of nocodazole inhibits but does not abolish all nuclear migration and that reversal results in the reestablishment of normal microtubule arrays and accelerated recovery of nuclear position. However, when the cells are exposed to higher concentrations of nocodazole, organized microtubule-containing structures are reestablished at reversal but they are abnormal

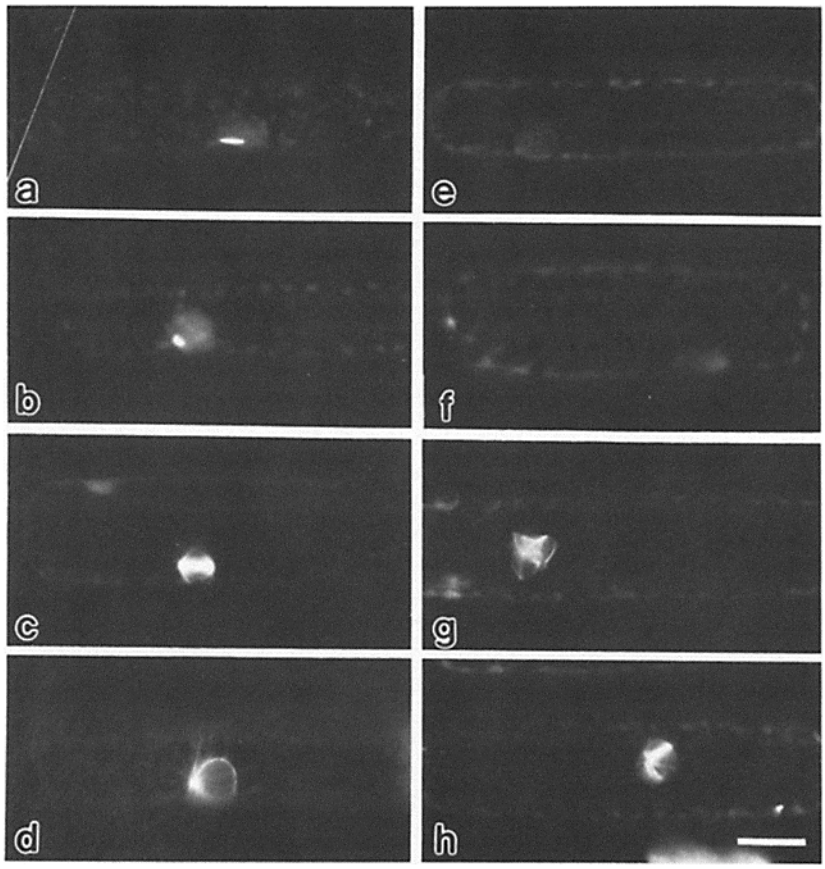

Figure 7. Antitubulin immunofluorescence of Nocodazole-treated cells. (*a* and *b*) Cells exposed to 2.5×10^{-8} M Nocodazole for 3 h. (*c* and *d*) 20 min after reversal from 2.5×10^{-8} M Nocodazole normal microtubule arrays are reestablished. (*e* and *f*) Cells exposed to 5.0×10^{-8} M Nocodazole for 3 h. (*g* and *h*) 20 min after reversal from 5.0×10^{-8} M Nocodazole, spindles have reformed but they are abnormal. Bar, 20 μm.

Table I. Nuclear Position and Location of Spindles in Cells Exposed to Nocodazole

	2.5×10^{-8} M Nocodazole		5×10^{-8} M Nocodazole	
Nuclear Position	R	R + 20 min	R	R + 20 min
			% cells	
Interphase	22	17	18	23
Migratory phase	38	17	81	75
Centered	41	66	1	3
Location of spindles				
			% spindles	
Interphase	—	0	—	0
Migratory phase	—	6	—	67*
Centered	—	54	—	2*
Total % spindles	—	60	—	69*

R, reversal time, the end of the 3-h exposure to nocodazole. At this time the drugged media was exchanged for fresh media.

Percentages refer to the proportion of cells with either nuclei, or metaphase and later-stage spindles at the position indicated in column one.

* Every spindle was splayed.

(see Fig. 7, *g* and *h*) and accelerated repositioning of the nuclei is not observed (Table I).

Uncoupling of Spindle Location from the Cleavage Furrow

In populations of cells that have been exposed to nocodazole, we find a substantial number of cells that contain spindles which are located at some distance from the center of the cell. Surprisingly, in these cells the cleavage furrow always forms in its normal location in the center of the cell. The cytoplasm is divided into two equal halves regardless of the location or the condition of the spindle. Fig. 8, *a* and *b*, shows two examples in which the position of the mitotic spindle is uncoupled from that of the cleavage furrow. In Fig. 8 *a*, the cell has been exposed to 2.5×10^{-8} M nocodazole and the spindle appears normal in every way except that it is displaced toward the hypothecal end of the cell. Fig. 8 *b* illustrates a similar situation except that the cell has been exposed to the higher drug concentration and contains an off-center, splayed spindle. In both situations the entire spindle is trapped in one of the daughter halves resulting in one daughter cell that has two nuclei (or many abnormal nuclei in the case of splayed spindles) and another which contains none (Fig. 8, *c* and *d*). Anucleate daughter cells do not construct a hypothecal cell wall and soon die. Finally, the spindles in Fig. 8, *a* and *b*, are at an earlier mitotic stage than one would expect to find in cells undergoing cytokinesis. It is possible that the timing of karyokinesis with respect to cytokinesis may also be partially uncoupled by nocodazole.

We used indirect immunofluorescence to compare the location of normal and splayed spindles between cells treated with the same two concentrations of nocodazole as in the previous experiments. The results are shown in Table I. 20 min after exposure to 2.5×10^{-8} M nocodazole, 60% of the cells contain mitotic spindles. The spindles are centrally located in 54% of the cells. The remaining 6% of the cells have spindles that appear normal, just like the centered spindles, yet they are located at some distance from the center of the cell. In cells exposed to the higher concentration of nocodazole, 69% of the cells contain mitotic spindles. 67% of the cells have off-center spindles and all of the spindles in the

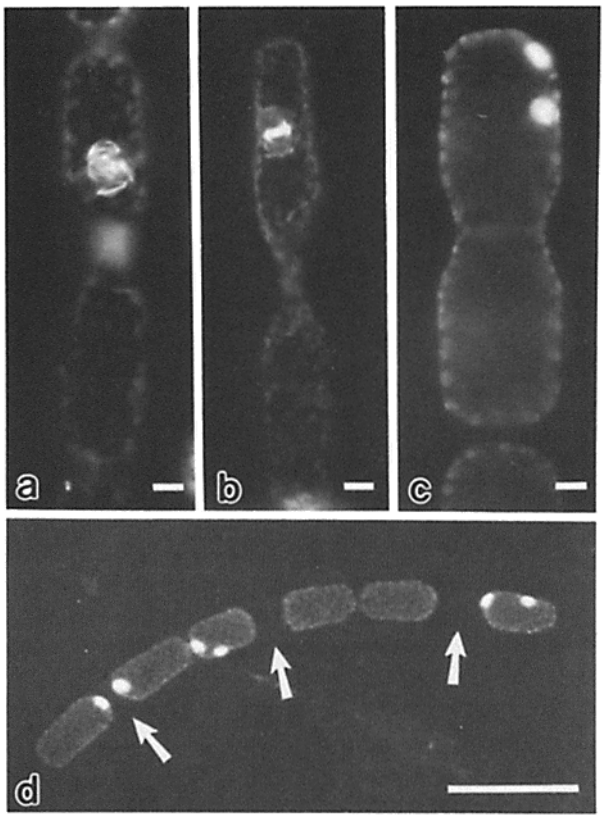

Figure 8. Nocodazole-induced uncoupling of spindle position from the cleavage furrow. (*a*) Antitubulin immunofluorescence showing a displaced, splayed spindle in a cleaving cell. (*b*) An off-center metaphase spindle during cleavage. (*c*) DAPI fluorescence microscopy of a cleaving cell with a displaced mitotic spindle. (*d*) A stand consisting of normal and binucleate/anucleate sister cell pairs. Arrows indicate the position of the most recent cleavage furrows. Bars, (*a–c*) 10 μm; (*d*) 100 μm.

population are splayed.

We have shown that accelerated nuclear repositioning occurs during reversal from exposure to 2.5×10^{-8} M nocodazole but that this does not occur after reversal from the higher drug concentration. The immunofluorescence results suggest that nuclear repositioning is dependent on the cell's ability to establish normal microtubule structures after nocodazole reversal. However, it appears that the location of the presumptive cleavage furrow is already determined by the time of mitosis and that its localization is independent of both the position of the dividing nucleus and the ability of the cell to reestablish normal microtubule structures after exposure to nocodazole.

Discussion

Nuclear Migration and Mitosis

During nuclear migration in *S. turris*, microtubules surround the nucleus and radiate out from an MTOC in close association with the center or leading edge of the cortical face of the migrating nucleus. Similar microtubule systems have been described in association with migrating nuclei in spores (2, 3), desmids (30, 34), diatoms (12, 35, 52, 53), mosses (45), and during pronuclear migration in sea urchins (4, 21, 25). Nuclear migration in many of these organisms has been shown to be sensitive to microtubule inhibitors (5, 28, 30, 43, 46, 56).

In *S. turris*, nuclear migration can be reversibly slowed or halted by exposure to low concentrations of nocodazole resulting in the disappearance of the cytoplasmic microtubule arrays. At reversal, the microtubule arrays reappear and the nuclei of the drugged population center themselves in an accelerated manner. The nuclei in cells that have been exposed to higher levels of nocodazole are not able to center themselves after reversal even though the microtubule arrays reappear. The appearance of splayed spindles suggests that these microtubule arrays have reformed abnormally. Staining patterns from splayed spindles using antibodies specific to spindle pole proteins indicate that the pole is disrupted with small pieces remaining at the tip of each splayed microtubule bundle. (Wordeman, L., and J. L. Salisbury, unpublished observations). Coss and Pickett-Heaps (11) have reported a similar effect in mitotic cells of the green alga *Oedegonium* in response to the herbicide isopropyl-*N*-phenyl carbamate. After reversal from isopropyl-*N*-phenyl carbamate exposure, the mitotic spindles reappear but they are oriented abnormally and many are multipolar. Spindles that are oriented at right angles to their normal axis often become trapped on one side of the cell wall resulting in binucleate/anucleate daughter cell pairs. In addition, there is ultrastructural evidence of pole fragmentation (11). These experiments suggest that although the microtubules reappear after exposure to microtubule inhibitors, the microtubule-organizing activity of the poles can be irreversibly disrupted. In the case of *S. turris*, the poles are disrupted by the higher concentration of nocodazole and this is correlated with improper positioning of the nucleus (Table I).

Our immunofluorescence studies and an excellent, high-resolution time-lapse film by the German Scientific Film Institute (22, 23) indicate that the spindle pole complex plays a dynamic role in the spatial redistribution of microtubules that are involved in nuclear positioning. Time-lapse films of dividing *S. turris* cells show fine fibers that pivot in the region of the pole and swing stiffly out from the central spindle back into the cytoplasm. This movement takes place at about the onset of anaphase. We believe that these fibers correspond to the peripheral microtubules seen in immunofluorescently stained cells. These microtubules are not equivalent to kinetochore microtubules and probably do not participate in chromosome-to-pole movement (McDonald, K., and W. Z. Cande, unpublished data). However, it is likely that they assist in the final stages of nuclear separation using a mechanism similar to nuclear migration and that they position the nuclei during and after cytokinesis.

Determination of the Division Site

In diatoms, cytokinesis occurs by furrowing and uses an actomyosin system for force generation (37, 48). This mechanism more closely resembles cleavage in animal cells rather than cell plate formation in plants (see reference 47 for review of animal cells; see reference 19 for review of plant cells). We examined the relationship between the position of the mitotic apparatus and the position of the cleavage furrow in *S. turris* using pulsed applications of nocodazole to inhibit nuclear migration. This treatment produces some cells with mitotic

nuclei that are displaced toward the hypothecal end of the cell. Interestingly, we found that the cleavage furrow always formed in the exact center of the cell regardless of the position of the spindle resulting in binucleate/anucleate daughter cells.

In animal cells, the position of the cleavage furrow appears to be dependent, at least until metaphase, on the position of the mitotic spindle (39). When the mitotic apparatus is displaced from its normal position, either by centrifugation (59), micromanipulation (9, 26), or mechanical deformation of the cell (40), the cleavage furrow bisects the mitotic spindle in its new location. Once furrowing has begun, however, it will proceed even if the mitotic apparatus is physically removed (24). A series of elegant experiments have demonstrated that furrow establishment in animal cells is intimately associated with apposing astral arrays (41, 42). In addition, it has been shown that disruption of the cell cortex with detergents will produce equal cell divisions in cells that possess unequally sizes asters and would normally have divided unequally (13, 51). Even though the mitotic apparatus does not appear to play a physical role in the furrowing process, the evidence suggests that astral microtubule arrays are used by the spindle during mitosis to establish areas of cortical differentiation that will determine the position of the cleavage furrow.

In the anastral cell divisions characteristic of higher plant cells, the localization of the plane of division is often subject to strict spatial and temporal regulation because successive planes of division can play an important role in plant morphogenesis (19). There are many indications that the location of the plane of division is determined before spindle formation presumably via some type of cortical determinant. In higher plants, for example, a band of microtubules (the preprophase band) that is parallel to the upcoming plane of division forms transiently before mitosis (8, 19, 55, 58). In addition, there are numerous cases in which the nuclei of plant cells migrate to a specific location before the onset of mitosis (2, 5, 19, 31, 52, 57). Also, in highly vacuolated plant cells, the nucleus moves from its peripheral location into the center of the cell along strands of cytoplasm. Several hours before prophase, these strands fuse and thicken selectively in one plane forming a plate called a phagmosome which predicts the future plane of division (19, 55). Finally, in the pennate diatoms the cleavage furrow is very long and narrow because it must bisect the cell's longitudinal axis. In these cells, furrowing begins early in prometaphase (36, 37).

Although the location of the division plane appears to be predetermined in many plant cells, it is often possible to alter the location of the cell plate or to establish auxillary cell walls by altering the position of the nucleus via centrifugation or drugs that inhibit nuclear migration (3, 5, 19, 31, 46, 54). In most cases, the timing of these manipulations with respect to that of mitosis critically affects the experimental results. Nevertheless these studies suggest that there is some interaction between the forming cell plate and the mitotic apparatus. In higher plants the cell plate forms by the coalescence of vesicles derived from the Golgi membrane–endoplasmic reticulum complex and is associated with an array of microtubules (phragmoplast microtubules) oriented perpendicular to the division plane. Some of these microtubules are derived from spindle microtubules and this may account for the cell plate abnormalities seen in cells with experimentally displaced mitotic nuclei (19).

In experiments involving short-term nuclear displacement, an attempt is usually made by the cell, using whatever cytoplasmic determinants of polarity it may possess, to correct the displacement before the onset of mitosis (3, 30–32, 46, 54). This is also the case in *S. turris*. During the 20-min period after nocodazole reversal, there is an abrupt increase in the number of cells with centered nuclei. However, a percentage of the nuclei do not reach the center of the cell before passing through karyokinesis. Unlike most plant and animal cells, in *S. turris* the displaced nuclei have absolutely no effect on the position or shape of the cleavage plane and there is no attempt to establish a new cleavage plane. It is more difficult to completely uncouple cytokinesis from karyokinesis in the cells of higher plants than it is in *S. turris*. This is probably due to the close interrelationship between the cell plate, phragmoplast, and the mitotic apparatus.

Although *S. turris* cleaves similarly to animal cells, it localizes the plane of division like a plant cell, presumably by using some type of cortical determinant, before the formation of the mitotic apparatus. The nature of this cortical determinant has not been established although microtubules have been implicated in this process. In higher plants, the preprophase band predicts the future position of the division plane and the final resting place of the migrating nucleus. Transmission electron microscopy reveals thickening of the cytoplasm and vesicles which cluster in this region when the preprophase band of microtubules appear (16). It is, however, unlikely that the preprophase band is the primary cortical determinant in this process because predetermination of the plane of division is accomplished in lower plants and algae (including *S. turris*) in the absence of this class of microtubules (7, 19). Misaligned cell plates are formed in *Allium* guard mother cells exposed to low levels of cytochalasin B, suggesting that actin is involved in the orientation of the cell plate in these cells (33). Also, phalloidin-specific staining has been localized in the cytokinetic apparatus of meristematic plant cells but not in the mitotic spindle or the preprophase band (10). However, so far we have found no electron microscopic or immunocytochemical evidence suggesting that midzone localization of actin is serving as a cue for the location of the cleavage plane in *S. turris*. The deposition and insertion of girdle bands in the cell's midzone is an early gross morphological event whose geometry resembles that of the future plane of division. Therefore, it is possible that in *S. turris*, predetermination of the future plane of division could be linked to girdle band deposition during interphase, or that both events require similar cortical determinants.

It is apparent, however, that for normal cell division in *S. turris* some interaction is necessary between the spindle and the cleavage furrow. To begin with, the nuclei must use some cortical guidance cue to migrate to the exact center of the cell, the future cleavage plane, in order to divide. Also, in time-lapse films the nuclei can be seen undergoing minor adjustments in position during and after cytokinesis presumably using the peripheral microtubule system (23). Lastly, in cells with displaced mitotic spindles, we see what appears to be temporal uncoupling of karyokinesis and cytokinesis as shown by the appearance of off-center metaphase spindles in cells undergoing cytokinesis.

Conclusion

In summary, we have demonstrated that nuclear migration and mitosis can be reversibly inhibited in *S. turris* by nocodazole in a dose-dependent manner concurrent with the disappearance of organized tubulin-containing structures. Also, using indirect immunofluorescence microscopy, we have documented the behavior of the peripheral microtubule system. This provides a striking illustration of pole-mediated regulation of microtubule distribution that does not appear to involve the polymerization and depolymerization of microtubules. Finally, we have shown that drug-induced inhibition of nuclear migration can uncouple karyokinesis from cytokinesis both spatially and temporally. Although cell division in *S. turris* resembles certain mechanochemical aspects of cleavage in animal cells, our evidence suggests that the spatial regulation of the cytokinetic apparatus relies on a mechanism of cortical determination that is characteristic of plant cells. The ease with which we can achieve complete uncoupling of karyokinesis from cytokinesis makes this organism unique. For this reason, *S. turris* is a useful experimental system for the study of nuclear and cytoskeletal function during cell division.

We thank Dr. Kevin Pfister for helpful discussions; Dan Coltrin, Doug Ohm, Troya Bogard, and Ellen Dean for excellent technical assistance; and Anna Astromov for initiating these studies.

This work was supported by grant GM23238 from the National Institutes of Health and grant PCM-8408594 from the National Science Foundation.

Received for publication 7 October 1985, and in revised form 3 January 1986.

References

1. Asai, D. J., C. J. Brokaw, W. C. Thompson, and L. Wilson. 1982. Two different monoclonal antibodies to tubulin inhibit the bending of reactivated sea urchin spermatozoa. *Cell Motil.* 2:599–614.

2. Bassel, A. R., C. C. Kuehnert, and J. H. Miller. 1981. Nuclear migration and asymmetric cell division in *Onoclea sensibilis* spores: an ultrastructural and cytochemical study. *Am. J. Bot.* 68:350–360.

3. Bassel, A. R., and J. H. Miller. 1982. The effects of centrifugation on asymmetric cell division and differentiation of fern spores. *Ann. Bot. (Lond.).* 50:185–198.

4. Bestor, T. H., and G. Schatten. 1981. Anti-tubulin immunofluorescence microscopy of microtubules present during the pronuclear movements of sea urchin fertilization. *Dev. Biol.* 88:80–91.

5. Brawley, S. H., and R. S. Quatrano. 1979. Effects of microtubule inhibitors of pronuclear migration and embryogenesis in *Fucus distichus* (Phaeophyta). *J. Phycol.* 15:266–272.

6. Britz, S. J. 1979. Chloroplast and nuclear migration. *In* Physiology of Movements. Encyclopedia of Plant Physiology, New Series, Vol. 7. W. Haupt and M. E. Feinleib, editors. Springer-Verlag, Berlin. 170–205.

7. Brown, R. C., and B. E. Lemmon. 1985. Preprophase establishment of division polarity in monoplastic mitosis of hornworts. *Protoplasma.* 124:175–183.

8. Busby, C. H., and B. E. S. Gunning. 1980. Observations of preprophase bands of microtubules in uniseriate hairs, stomatal complexes of sugar cane, and *Cyperus* root meristems. *Eur. J. Cell Biol.* 21:214–223.

9. Carleson, G. J. 1952. Microdissection of the dividing neuroblast of the grasshopper *Chortophaga viridifasciata* (de Geer). *Chromosoma (Berl.).* 5:199–220.

10. Clayton, L., and C. W. Lloyd. 1985. Actin organization during the cell cycle in meristematic plant cells. *Exp. Cell Res.* 156:231–238.

11. Coss, R. A., and J. D. Pickett-Heaps. 1974. The effects of isopropyl-*N*-phenyl carbamate on the green alga *Oedogonium cardiacum*. I. Cell division. *J. Cell Biol.* 63:84–98.

12. Crawford, R. M. 1973. The protoplasmic ultrastructure of the vegetative cell of *Melosira varians*. *J. Phycol.* 9:50–61.

13. Dan, K., S. Endo, and I. Uemura. 1983. Studies on unequal cleavage in sea urchins. II. Surface differentiation and the direction of nuclear migration. *Dev. Growth & Differ.* 25:227–237.

14. Dawson, P. J., J. S. Hume, and C. W. Lloyd. 1985. Monoclonal antibody to intermediate filament antigen cross-reacts with higher plant cells. *J. Cell Biol.* 100:1793–1798.

15. DeMey, J., A. M. Lambert, A. S. Bajer, M. Moeremans, and M. DeBrabander. 1982. Visualization of microtubules in interphase and mitotic plant cells of *Haemanthus* endosperm with the immunogold staining (IGS) method. *Proc. Natl. Acad. Sci. USA.* 79:1898–1902.

16. Galatis, B., and K. Mitrakos. 1979. On the differential divisions and preprophase microtubule bands involved in the development of stomata of *Vigna sinensis L. J. Cell Sci.* 37:11–37.

17. Green, P. B. 1984. Shifts in plant cell axiality: histogenetic influences on cellulose orientation in the succulent *Graptopetalum*. *Dev. Biol.* 103:18–27.

18. Guillard, R. R. L. 1975. Culture of phytoplankton for feeding marine invertebrates. *In* Culture of Marine Invertebrate Animals. W. Smith and H. Chanley, editors. Plenum Publishing Corp., New York. 29–60.

19. Gunning, B. E. S. 1982. The cytokinetic apparatus: its development and spatial regulation. *In* The Cytoskeleton in Plant Growth and Development. C. W. Lloyd, editor. Academic Press, Ltd. London. 229–292.

20. Hardham, A. R. 1982. Regulation of polarity in tissues and organs. *In* The Cytoskeleton in Plant Growth and Development. C. W. Lloyd, editor. Academic Press, Ltd. London. 377–403.

21. Harris, P., M. Osborn, and K. J. Weber. 1980. Distribution of tubulin-containing structures in the egg of the sea urchin *Strongylocentrotus purpuratus* from fertilization to first cleavage. *J. Cell Biol.* 84:668–679.

22. Heunert, H.-H. 1975. Diatoms from the sea. Methods of study and life cycle. I. Methods of vegetative reproduction. *Mikrokosmos.* 64:357–336.

23. Heunert, H.-H. Ungeschlechtliche Fortplanzung der Kieselalge *Stephanopyxis turris*: C 982 T. Institut fur den Wissenschaftlichen Film, Gottingen, Nonnenstieg 72.

24. Hiramoto, Y. 1971. Analysis of cleavage stimulus by means of micromanipulation of sea urchin eggs. *Exp. Cell Res.* 68:291–298.

25. Hollenbeck, P. J., and W. Z. Cande. 1985. Microtubule distribution and reorganization in the first cell cycle of fertilized eggs of *Lytechinus pictus*. *Eur. J. Cell Biol.* 37:140–148.

26. Kawamura, K. 1960. Studies on cytokinesis in neuroblasts of the grasshopper *Chortophaga viridifasciata* (de Geer). II. The role of the mitotic apparatus in cytokinesis. *Exp. Cell Res.* 21:9–18.

27. Li, C.-W., and B. E. Volcani. 1984. Aspects of silification in wall mophogenesis of diatoms. *Philos. Trans. R. Soc. Lond. B Biol. Sci.* 304:811–847.

28. Mar, H. 1980. Radial cortical fibers and pronuclear migration in fertilized and artificially activated eggs of *Letichinus pictus*. *Dev. Biol.* 78:1–13.

29. Marchant, H. J. 1982. The establishment and maintenance of plant cell shape by microtubules. *In* The Cytoskeleton in Plant Growth and Development. C. W. Lloyd, editor. Academic Press, Ltd. London. 296–319.

30. Meindl, U. 1983. Cytoskeletal control of nuclear migration and anchoring in developing cells of *Micrasterias denticulata* and the change caused by the anti-microtubule herbicide amiprophos-methyl (APM). *Protoplasma.* 118:75–90.

31. Mineyuki, Y., and M. Furuya. 1980. Effect of centrifugation on the development and timing of premitotic positioning of the nucleus in *Adiantum* protonema. *Dev. Growth & Differ.* 22:867–874.

32. Ota, T. 1961. The role of the cytoplasm in cytokinesis in plant cells. *Cytologia.* 26:428–447.

33. Palevitz, B. A., and P. K. Hepler. 1974. The control of division during stomatal differentiation in *Allium*. II. Drug studies. *Chromosoma (Berl.).* 46:327–341.

34. Pickett-Heaps, J. D., and L. C. Fowke. 1970. Mitosis, cytokinesis, and cell elongation in the desmid *Closterium littorale*. *J. Phycol.* 6:189–215.

35. Pickett-Heaps, J. D., K. L. McDonald, and D. H. Tippit. 1975. Cell division in the pennate diatom *Diatoma vulgare*. *Protoplasma.* 86:205–242.

36. Pickett-Heaps, J. D., D. H. Tippit, and J. A. Andreozzi. 1978. Cell division in the pennate diatom *Pinnularia*. I. Early stages in mitosis. *Biol. Cell.* 33:71–78.

37. Pickett-Heaps, J. D., D. H. Tippit, and J. A. Andreozzi. 1978. Cell division in the pennate diatom *Pinnularia*. II. Later stages in mitosis. *Biol. Cell.* 33:79–84.

38. Porter, K. R. 1973. Microtubules in intracellular locomotion. *Ciba Found. Symp.* 14:149–169.

39. Rappaport, R. 1971. Cytokinesis in animal cells. *Int. Rev. Cytol.* 31:169–213.

40. Rappaport, R., and B. N. Rappaport. 1974. Establishment of cleavage furrows by the mitotic spindle. *J. Exp. Zool.* 189:189–196.

41. Rappaport, R., and B. Rappaport. 1983. Cytokinesis: effects of blocks between the mitotic apparatus and the surface on furrow establishment in flattened echinoderm eggs. *J. Exp. Zool.* 227:213–227.

42. Rappaport, R., and B. N. Rappaport. 1984. Division of constricted and urethane-treated sand dollar eggs: a test of the polar stimulation hypothesis. *J. Exp. Zool.* 231:81–92.

43. Schatten, G., and H. Schatten. 1981. Effects of motility inhibitors during sea urchin fertilization. *Exp. Cell Res.* 135:311–330.

44. Schmid, A.-M. M. 1980. Valve morphogenesis in diatoms: a pattern-related filamantous system in pennates and the effect of APM, colchicine, and osmotic pressure. *Nova Hedwigia.* 33:811–847.

45. Schmiedel, G., and E. Schnepf. 1979. Side branch formation and orien-

tation in the caulonema of the moss *Funaria hygrometrica*: normal development and fine structure. *Protoplasma.* 100:367–383.

46. Schmiedel, G., and E. Schnepf. 1979. Side branch formation and orientation in the caulonema of the moss *Funaria hygrometrica*: experiments with inhibitors and with centrifugation. *Protoplasma.* 101:47–59.

47. Schroeder, T. E. 1975. Dynamics of the contractile ring. *In* Molecules and Cell Movement. S. Inoué and R. E. Stephens, editors. Raven Press, Inc., New York. 305–332

48. Soranno, T., and J. D. Pickett-Heaps. 1982. Directionally controlled spindle disassembly after mitosis in the diatom *Pinnularia. Eur. J. Cell Biol.* 26:234–243.

49. Spiegelman, B. M., M. A. Lopata, and M. W. Kirschner. 1979. Aggregation of microtubule initiation sites preceding neurite outgrowth in mouse neuroblastoma cells. *Cell.* 16:253–263.

50. Stosch, H. A. v., and G. Drebes. 1964. Entwicklungsgeschichtliche untersuchungen an zentrischen diatomeen IV. Die plankton-diatomee *Stephanopyxis turris*—ihre behandlung und entwicklungsgeschichte. *Helgol. Wiss. Meeresunters.* 2:209–257.

51. Tanaka, Y. 1976. Effects of the surfactants on the cleavage and further development of the sea urchin embryos. I. The inhibition of micromere formation at the fourth cleavage. *Dev. Growth & Differ.* 18:113–122.

52. Tippit, D. H., K. L. McDonald, and J. D. Pickett-Heaps. 1975. Cell division in the centric diatom *Melosira varians. Cytobiologie.* 12:52–73.

53. Tippit, D. H., and J. D. Pickett-Heaps. 1977. Mitosis in the pennate diatom *Surirella ovalis. J. Cell Biol.* 73:705–727.

54. Van Wisselingh, K. 1909. Zur physiologie der spirogyrazelle. *Beih. Bot. Centralbl.* 24:133–210.

55. Venverloo, C. J., P. H. Hovenkamp, A. J. Weeda, and K. R. Libbenga. 1980. Cell division in *Nautilocalyx* explants. I. Phragmosome, preprophase band and plane of division. *Z. Pflanzenphysiol.* 100:161–174.

56. Vogelmann, Th. C., A. R. Bassel, and J. H Miller. 1981. Effects of microtubule inhibitors on the nuclear migration and rhizoidal differentiation in germinating fern spores (*Onoclea sensibilis*). *Protoplasma.* 109:295–316.

57. Wada, M., Y. Mineyuki, A. Kadota, and M. Furuya. 1980. The changes of nuclear position and distribution of circumferentially aligned cortical microtubules during the progression of the cell cycle in *Adiantum* protonema. *Bot. Mag. Tokyo.* 93:237–245.

58. Wick, S. M., R. W. Seagull, M. Osborn, K. Weber, and B. E. S. Gunning. 1981. Immunofluorescence microscopy of organized microtubule arrays in structurally stabilized meristematic plant cells. *J. Cell Biol.* 89:685–690.

59. Yamamoto, M. 1964. Note on the effect of centrifugal force upon the cleavage on sea urchin egg with special reference to the position of the mitotic apparatus and the formation of the furrow. *Sci. Rep. Tohoku Univ. Fourth Ser. (Biol.).* 30:187–195.